World Journal of Chemistry 7 (2): 34-41, 2012
ISSN 1817-3128

DOI: 10.5829/idosi.wjc.2012.7.2.1103

Synthesis, Modification and Characterization of Single and Mixed Phase Titania Prepared by Microwave Assisted Sol Gel Method

[1]Gamil A. El-Shobaky, [2]Hassan M.A. Hassan, [3]Khaled S. Abdel Halim, [4]Sabary A. El-Korashy and [2]Shaimaa K. Mohamed

[1]Physical Chemistry Department, National Research Center, Giza, Egypt
[2]Chemistry Department, Faculty of Science, Suez Canal University, Suez, Egypt
[3]Central Metallurgical Research & Development Institute, Egypt
[4]Chemistry Department, Faculty of Science, Suez Canal University, Ismaillia, Egypt

Abstract: Single and mixed phase titania was synthesized by microwave assisted sol gel method. Ceria modified titania was prepared by deposition- precipitation (DP) method followed by microwave irradiation for 2 minutes. The prepared solids were characterized by X-ray powder diffraction (XRD), N_2 adsorption-desorption, scanning electron microscopy (SEM) and transmission electron microscopy (TEM) techniques. The effects of the phase composition and modification with ceria on the structural, surface and texture properties of the prepared titania were studied. Adsorption and photocatalytic degradation of methylene blue (MB) dye under UVA irradiation over the prepared solids were performed. The crystallite sizes of the prepared solids were lower than 10 nm and have high specific surface areas and possessed mesoporous structures. The mixed phase titania showed better adsorption for MB dye and exhibited higher intrinsic photocatalytic activity. Ceria modified titania exhibited higher photocatalytic activity than the pure titania and the reasons were discussed. The microwave assisted sol gel method adopted in this study, besides saving time and energy, allowed the control of phase composition and crystallite size of titania and led to better adsorptive properties for MB.

Key words: Microwave irradiation · Ceria · Titania · Methylene blue · Photocatalysis

INTRODUCTION

TiO_2 is one of the most widely utilized photocatalysts for environmental applications due to its strong photo-oxidative power, non-toxicity, chemical stability and relatively low-cost compared to other catalysts. Nanostructured TiO_2 is highly photoactive and is widely used in different fields including photovoltaics, photocatalysts, catalysis, gas sensors, antifogging and self-cleaning coatings, gate insulator for devices and Li batteries [1]. Upon band gap excitation of TiO_2, the photoinduced electrons and positively charged holes can reduce and oxidize the species adsorbed on the semiconductor particles. The high degree of recombination between photo- generated electrons and holes is a major rate-limiting factor controlling the photocatalytic efficiency [2]. It is well known that the composite of two kinds of semiconductors or two phases of the same semiconductor is beneficial in reducing the combination of photo-generated electrons and holes and enhancing photocatalytic activity [3]. In particular, the anatase/rutile TiO_2 heterogeneous nanostructure is intriguing because it involves only a change in the crystal structure of the same material. In fact, a synergistic effect has been proposed for the high photocatalytic activity of Degussa P25 TiO_2, which contains both anatase and rutile. The coupling of anatase and rutile phase TiO_2 allows the transfer of electrons excited by ultraviolet light from anatase to rutile TiO_2 as a result of the slightly lower conduction band energy of the rutile phase and thus charges recombination can be suppressed [4]. Also, Rare-earths can be employed as electron acceptors to enhance the quantum efficiency of TiO_2 by either increasing the electron density imparted to TiO_2 surface or expanding the light absorption range [5, 6]. Therefore, it is of prime importance to develop effective techniques to fabricate such heterogeneous nanostructures [4].

Corresponding Author: Gamil A. El-Shobaky, Physical Chemistry Department, National Research Center, Giza, Egypt.

The applications of TiO_2 strongly depend on its physicochemical properties [7], e.g. crystallinity, grain size, pores, surface area [8] and phase composition, which are highly influenced by the preparation method, experimental parameters and heat treatment. Among the various preparation methods for nanosized TiO_2, the sol-gel process has the advantages of high purity in comparison with sulfate or chloride processes and easy application to thin film processes. In the sol-gel method, particle size and the phases of resultant TiO_2 can be successively controlled by changing the experimental parameters [9]. Recently, microwave synthesis of nano-sized materials attracted much attention in the preparation of catalysts [7, 10-15]. Microwave irradiation furnishes energy to the reactants by means of molecular interaction with the electromagnetic field; the rapid and uniform generation of heat allows the achievement of equilibrium between the bulk and the surface of the material more quickly than with conventional thermal treatment [11]. The other advantages of microwave heating include promotion of fine microstructures, alteration of phase transformation behavior [16] and suppression of grain growth. Besides, it can alter the activity and selectivity in certain reactions. Murugan *et al.* [10] obtained anatase TiO_2 powder by microwave hydrothermal method for 3 min. Addamo *et al.* [11] found that using of microwaves for a very short time enhanced the TiO_2 crystallinity, prevented the increase of particle size and minimized the decrease of specific surface area. Li *et al.* [7] synthesized Anatase TiO_2 nanocrystal colloids with high dispersion and photocatalytic activity from peroxo-titanium-acid precursor by microwave assisted hydrothermal method within 30 min at low temperature.

The present work is designated to synthesize single and mixed phase titania by a simple energy and time saving technique, namely, microwave assisted sol gel method. The effect of the phase composition on the structural, surface, texture and redox properties of the prepared titania is studied. Also, modification of titania by another n-type semiconductor (ceria) is performed. Ceria modified titania is prepared by deposition- precipitation (DP) method followed by microwave irradiation instead of conventional thermal treatment. MB, a commonly used pollutant dye, is chosen as a model pollutant dye to investigate the adsorptive properties and the photocatalytic activities of the prepared nano-sized catalysts.

MATERIALS AND METHODS

Materials: Cerium nitrate hexahydrate Ce $(NO_3)_3 6H_2O$ (99%) andtitanium iso-propoxide (98%) were supplied by Sigma-Aldrich company. The precipitating agents were 25% aqueous NH_3 and 4M NaOH (Fisher-Scientific). All chemicals are used without any further purification.

Catalyst Preparation: TiO_2 was prepared by hydrolysis of 10 ml of titanium iso-propoxide in 100 ml of ethanol: water (1:1) mixture for 30 minutes under continuous stirring. The formed precipitate was filtered and washed with distilled water. The precipitate was then slowly dissolved in 50 ml HNO_3: H_2O mixture (1:1) (*procedure I*) or in 100 ml HNO_3: H_2O mixture (1:1) (*procedure II*) with continuous stirring for 10 minutes resulting in a clear solution. The solution was immediately transferred to a domestic microwave oven and irradiated for 30 minutes which resulted in a white colloidal precipitate. Ammonia solution was added till pH 10 andthe precipitate was subjected again to microwave irradiation for 30 minutes. The prepared TiO_2 was collected by filtration, washed with distilled water and left to dry at 120°C for 6 h. The titania obtained from *procedure I* has an off-white color where the titania obtained from *procedure II* has a white color. The CeO_2/TiO_2 catalysts, containing 10 wt. % CeO_2, were prepared using DP method. A known amount of cerium nitrate was added at room temperature to the suspension of TiO_2 from the two procedures. 4M NaOH was added dropwise with continuous stirring until the pH of the resulting solution attained ~ 10. The resulting solution was then placed in a conventional microwave. The microwave power was set to 80% of 1000 W and operated in 30-s cycles (on for 10 s, off for 20 s) for 2 minutes. The resulting yellow powder was carefully washed with distilled water and dried at 90°C.

Characterization: Phase identification and crystallite size of different phases present in the produced powders were performed at room temperature using X-ray diffraction (XRD, Bruker axs D8, Germany) with Cu-Kα (λ= 1.5406 Å) radiation and secondly monochromator in the range 2θ from 10? to 80?. Crystallite size is automatically calculated from XRD data using the diffraction peaks and computer software TOPAS2. The relative abundance of anatase phase of TiO_2 to rutile in the samples was calculated by using the following equation [6]:

$$F_r = 1.26\ I_r \backslash (I_a + 1.26\ I_r)$$

Where F_r is the rutile fraction and I_i and I_a are the strongest intensities of the rutile (110) and anatase (101) diffraction angles, respectively. The peak area of the main diffraction line was considered as a quantitative measure for the degree of crystallinity of the phase present. Specific surface area (S_{BET}), total pore volume (V_p) andpore size distribution of the samples were determined by BET surface area analyzer (Nova 2000 series, Quantachrome Instruments, UK). The BET approach using adsorption data over the relative pressure ranging from 0.05 to 0.3 was utilized to determine specific surface area. The values of V_p were estimated from nitrogen adsorption-desorption isotherm at a relative pressure of 0.99. The most frequent pore width was measured from pore size distribution curves. Prior to analysis, the samples were outgassed at 200°C and pressure of 10^{-5} Torr for 5 h. The size and morphology of the investigated catalysts were characterized using scanning electron microscope (SEM, JEOL-JSM-5410, Japan) and transmission electron microscopy (TEM), JEM-1230 (JOEL) operated at 120 kV. For the TEM imaging, the sample powder was dispersed in methanol by using ultrasonic radiation for 5 minutes and deposited onto the carbon-coated copper grids.

Photocatalytic Activity Measurements: The measurements were performed at room temperature as followed: 100 mg of the photocatalyst was added to a 250 ml beaker containing 100 ml of MB solution (4×10^{-5} mol/l). The solution was kept in dark under continuous stirring for 30 minutes in order to obtain adsorption/desorption equilibrium. A UV lamp (Handheld UV Lamp, LW/SW, 6W, UVGL-58, UVP, Inc.) positioned over the beaker was used as a light source to trigger the photocatalytic reaction.

The MB solution was irradiated for 120 minutes using long wave UV (UVA, 365 nm). 5 ml of the solution was withdrawn every 20 minutes and centrifuged. The concentration of MB solution was determined using an UV– visible spectrophotometer (A Shimadzu-1601PC UV-Visible automatic recording spectrophotometer).

RESULTS AND DISCUSSION

Structural Characterization: Figure 1 depicts the X-ray diffractograms of the TiO_2 obtained from procedure I and procedure II. It could be observed that the prepared TiO_2 (procedure I) existed as a mixture of anatase (JCPDS 21-1272) and rutile (JCPDS 77-0443) phases and it will be referred to as TiO_2(R+A). The anatase to rutile ratio was found to be 0.61. The obtained powder from procedure II existed as anatase phase only (JCPDS 21-1272) and will be referred to as TiO_2 (A). The crystallite size, the relative abundance of phases and the degree of crystallinity of TiO_2 phases present in the obtained powders are given in Table 1.

The phase transformation process from anatase to rutile has been widely studied for both scientific and application-driven reasons because the TiO_2 phase is one of the critical factors for many applications [1]. Experimentally, factors such as particle size and morphology, surface chemistry, concentration of intrinsic defects and impurities andtemperature have been observed to influence the transformation [17]. Ding *et al.* [1] investigated the phase transformation from anatase to rutile phase and proposed a simple model to describe the phase transformation process considering that

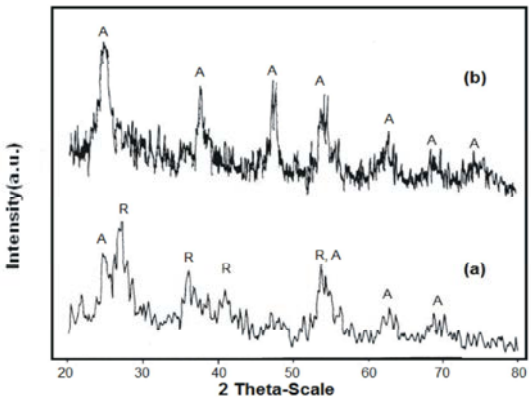

Fig. 1: X-rays diffractograms of the prepared titania (a) obtained from procedure I and (b) obtained from procedure II. A: Anatase phase and R: Rutile phase

Table 1: The structural properties of the prepared titania

	The relative abundance of phases		Crystallite size (nm)		Degree of crystallinity (a.u.)	
Items	Anatase	Rutile	Anatase	Rutile	Anatase	Rutile
Procedure I	38%	62%	9	4	6.2	7.9
Procedure II	100%	-	3	-	9.6	-

the nucleation and growth of rutile phase were determined by the aggregation manner of anatase nano-crystals and Ostwald ripening process, respectively. They found that the anatase to rutile phase transformation process was accelerated at higher temperature, high solution acidity and higher precursor concentrations. Cheng *et al.* [18] and Zheng *et al.* [19] studied the influence of $TiCl_4$ concentration on the hydrothermal synthesis of TiO_2 particles and found that high $TiCl_4$ concentration facilitated the anatase to rutile phase transformation process.

The model of anatase to rutile transformation proposed by Ding *et al.* [1] can be used to explain the results obtained in this study. It can be seen that the concentration of Ti precursor during the first stage of microwave irradiation employed in procedure I was higher than that in procedure II by a factor of 2. This high concentration of Ti precursor increased the aggregation of anatase nano-crystals formed in the solution which led to the formation of rutile nuclei at the interface between anatase nano-crystals. Once the stable rutile nuclei are formed, it rapidly amasses the surrounding atoms [17]. On the other hand, it could be seen that the crystallite size of anatase obtained from procedure II, i.e. 3 nm, was lower than the critical size at which rutile is preferred over anatase. At this crystallite size the anatase phase is the thermodynamically preferred phase which is in agreement with the results cited in literature [17]. The obtained results assert the importance of microwave irradiation in

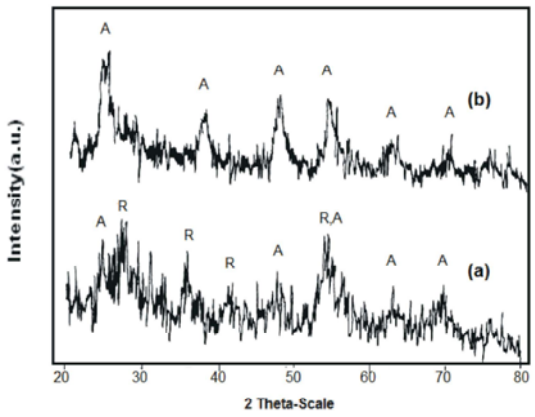

Fig. 2: X-rays diffractograms of the prepared ceria/titania (a) CeO_2/TiO_2 (R+A) and (b) CeO_2/TiO_2 (A). A: Anatase phase and R: Rutile phase

the synthesis of nano- sized metal oxides. In solid state reaction, the transformation of anatase to rutile is observed over the temperatures range 600-1000°C [1]. The high calcinations temperatures causes' large crystal growth of the titania phases. But when microwave assisted sol gel method was used, the two titania phases can be formed with significantly lower crystallite sizes. Fig. 2, depicts the X-ray diffractograms of the prepared CeO_2/TiO_2 (R+A) and CeO_2/TiO_2 (A) solids. For both solids, no peaks corresponding to ceria were found in the diffractograms which may suggest the presence of ceria in highly dispersed state and/or the possible formation of

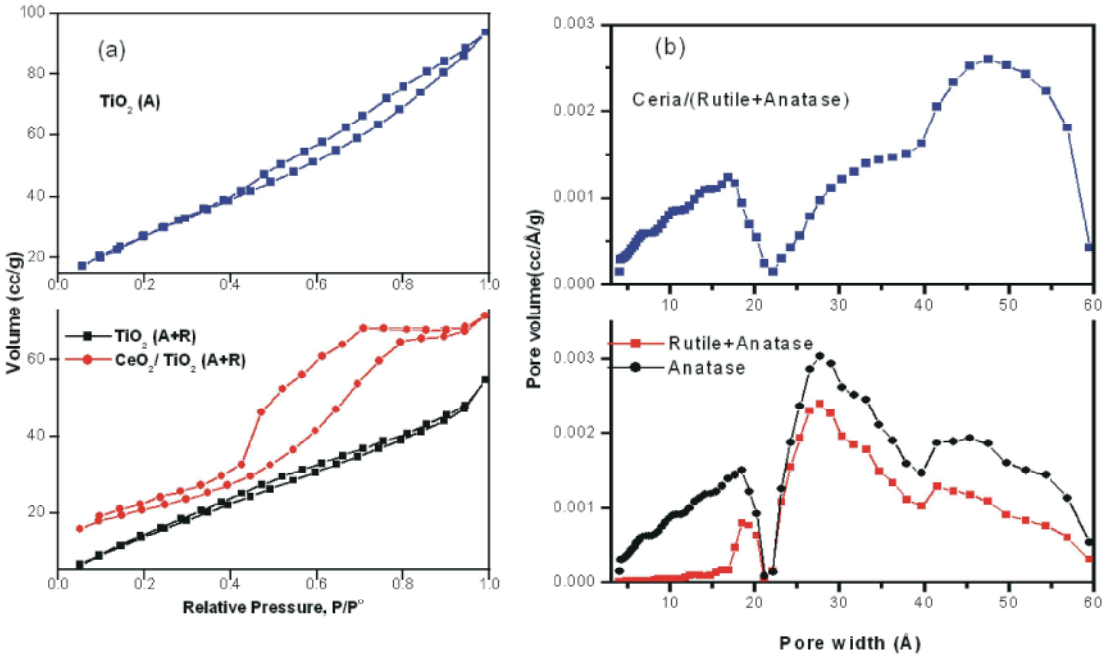

Fig. 3: (a) N_2 adsorption-desorption isotherms conducted at -196°C and (b) Pore size distribution curves.

Table 2: The surface characteristics of titania and ceria modified titania.

Sample	S_{BET} (m^2/g)	V_p (cm^3/g)	Pore width(nm)
TiO_2(A)	110	0.144	2.7
TiO_2(R+A)	69	0.084	2.7
CeO_2/TiO_2(R+A)	74	0.110	4.7

ceria-titania solid solution. Because of the relatively large size mismatch with Ti^{4+} (0.68Å) cations, Ce^{3+}/Ce^{4+} (1.03/1.02 Å) are not expected to occupy the titanium sites in the lattice of titania. It is more likely that they stay on the particle surfaces and at grain boundaries and grain junctions thus inhibiting crystallite growth of titania through the formation of Ce-O-Ti bonds [5]. Considering the ionic radii, of Ce^{3+}/Ce^{4+} and Ti^{4+} andthe method of preparation adopted in this study, the possibility of formation of ceria-titania solid solution was neglected.

Surface and Textural Characterization: Nitrogen adsorption–desorption isotherms conducted at -196°C over the prepared titania and ceria modified titania are shown in Fig. 3. The obtained isotherms belong to type IV isotherms according to IUPAC classification and exhibited hysteresis loops which are characteristic of mesoporous solids. Both TiO_2(R+A) and TiO_2(A) solids show Type H3 loop which is usually assigned to slit-shaped pores due to non-rigid aggregates of particles. CeO_2/TiO_2(R+A) shows type H2 loop according to IUPAC classification which indicate that the pore structure is complex and tend to be made up of interconnected networks of pores of different size and shape.

The different surface characteristics of the investigated solids are cited in Table 2. Examination of Table 2 shows the following: (i) Both the specific surface area (S_{BET}) and total pore volume (V_p) values of titania (A) are higher than those measured for the mixed phase titania. This can be explained by the fact that rutile usually has lower specific surface area than that reported for anatase [17] andsince the TiO_2(R+A) has a higher content of rutile phase relative to anatase phase, then it is expected to show lower specific surface area. (ii) The ceria loading slightly increased the value of surface area which attained 7%. This is consistent with the results reported by Zhu *et al.* [20]. (iii) The total pore volume observed for CeO_2/TiO_2(R+A) was 31% greater than that observed for TiO_2(R+A) which pointed to the presence of larger number of mesopores in the structure of the former. (iv) The pore width of the investigated samples is in the range of 2.7– 4.7 nm which confirm the nature of the prepared system as mesoporous solids.

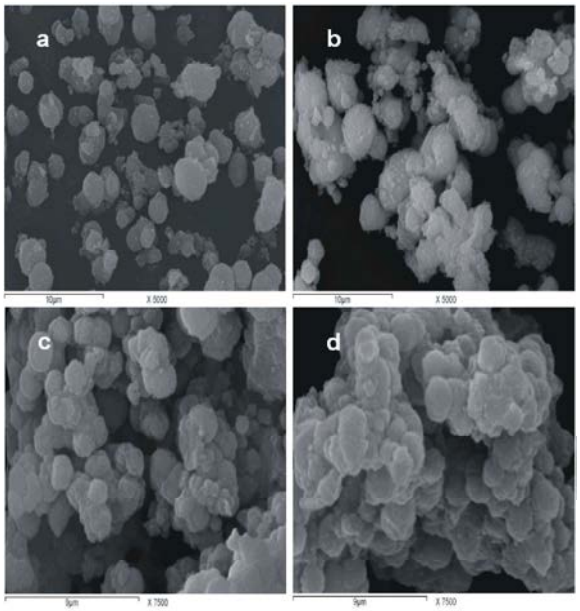

Fig. 4: SEM images of (a) TiO_2 (A), (b) CeO_2/TiO_2 (A), (c) TiO_2(R+A) and (d) CeO_2/TiO_2(R+A)

The pore size distribution curves of the prepared solids are shown in Fig. 3. The pore size distribution curves of both TiO_2 solids can be identified as a trimodal distribution. The micropore portion of anatase is bigger than that of the mixed phase titania which may lead to the bigger surface area of the former. The pore size distribution curve of CeO_2/TiO_2 (R+A) can be clearly identified as a bimodal distribution of micropores of about 0.4 – 2 nm and mesopores of the range of 2.1 - 6 nm. It may be concluded that doping with ceria led to enlargement of the pore width. SEM images of TiO_2 (A), TiO_2 (R+A), CeO_2/TiO_2 (A) and CeO_2/TiO_2 (R+A) are given in Fig. 4. The SEM image of TiO_2 (A) shows well dispersed spherical particles having diameters ranging from 0.8 to 2.6 µm. After modification with ceria, some aggregation of the spherical particles occurs. The SEM images of TiO_2 (R+A) and CeO_2/TiO_2 (R+A) show aggregation of spherical particles having diameters ranging from 0.7 to 1.6 µm and small irregular voids distributed among the particles.

TEM and HRTEM images of titania and ceria modified titania is given in Fig. 5. The TEM image of TiO_2(R+A) shows closely aggregated nanoparticles having diameters in the range of 4 - 8 nm, which is well consistent with the results obtained from XRD analysis. Clear lattice fringes are observed in the HRTEM image CeO_2/TiO_2(R+A) and the presence of dark and light intermittent bands observed in the image could be due to

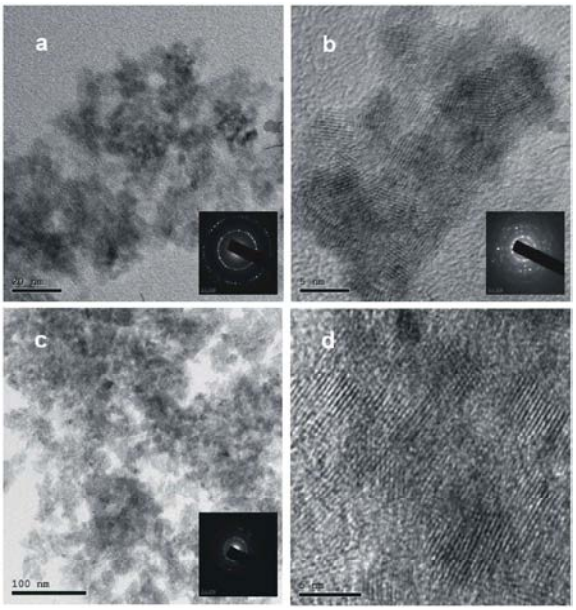

Fig. 5: TEM images observed for (a) TiO_2(R+A) and (c) TiO_2 (A) and HRTEM of (b) CeO_2/TiO_2(R+A) and (d) TiO_2 (A). Insets are the selected area of electron diffraction

diffraction phenomenon caused by the superimposition of CeO_2 and TiO_2 grains. The TEM image of TiO_2 (A) shows closely aggregated nanoparticles having diameters in the range of 2 - 5 nm, which is well consistent with the results obtained from XRD analysis.

Adsorption and Photocatalytic Degradation of MB Dye: The photocatalytic activity of the prepared catalysts was elucidated by the photocatalytic degradation of MB dye in aqueous solution. Before UV illumination of the MB solution, the solution was kept with the catalysts in dark in order to achieve adsorption/desorption equilibrium and to study the adsorption of MB on the prepared catalysts. Adsorption of MB dye in dark and photocatalytic degradation of MB dye under UVA illumination of titania and ceria modified titania as a function of time are shown in Fig.6 a. From this Fig., it can be seen that the adsorption of MB dye by the mixed phase titania is much better than that of anatase. Also, the adsorption of the dye was greatly enhanced by modifying anatase with ceria. However, an opposite effect occurred when the mixed phase was modified with ceria. It is interesting to note that although the specific surface area of TiO_2 (R+A) is lower than that of anatase, its adsorptive property is much higher than that of anatase. This may be related to the electrical charge of the solid surface. It is generally believed that the emerging of negative charges at the surface of solids improves the adsorption of cationic MB species [21,22]. Thus it may be concluded that, mixing of anatase and rutile on the atomic level as in the case of TiO_2 (R+A) might generate strong negative adsorption sites for the dye. The observed significant adsorption capacity of the employed systems might suggest their use as effective adsorbents and photocatalysts.

The photocatalytic activity of titania and ceria modified titania for the degradation of MB dye under UVA illumination is shown in Fig. 6b. From this Fig., it can be seen that pure single and mixed phase titania catalysts showed quite similar photocatalytic behavior. The photocatalytic degradation of MB is a first order reaction and its kinetics may be expressed as ($\ln C_o/C_t = k\ t$) where k is the apparent rate constant, C_o and C_t are the initial concentration and concentration at different time intervals of MB, respectively. The values of k were calculated for TiO_2(R+A) and TiO_2 (A) and were found to be 0.1085 and 0.1166 $min^{-1}g^{-1}$, respectively. However, in comparing different catalysts, it is necessary to know the extent to which a change in catalytic activity is caused by a change in the specific surface area of the catalyst, in contrast to a change in intrinsic reactivity.

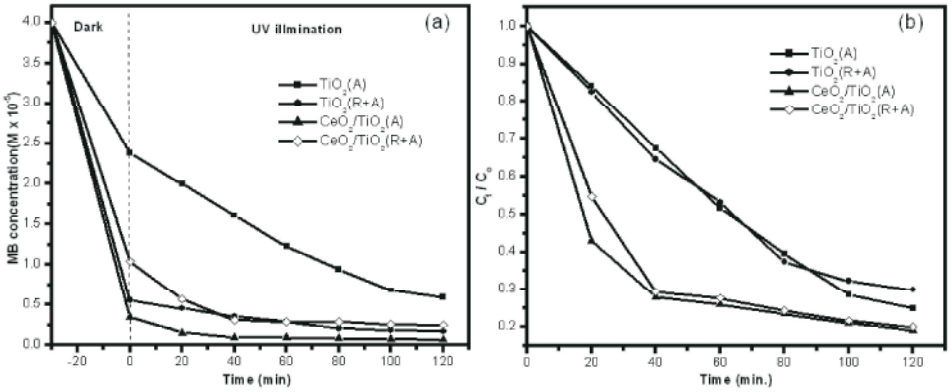

Fig. 6: Adsorption and photocatalytic performance of titania and ceria modified titania for the degradation of MB dye

Thus, the rate constant per unit surface area (k`, min/m^2) was calculated for each catalyst and the values were 1.57 x $10^{-3}$for TiO_2(R+A) and 1.06 x 10^{-3} for TiO_2 (A). It can be seen that the mixed phase titania possessed higher intrinsic catalytic activity than anatase which is due to synergistic effect between rutile and anatase. Treating with ceria greatly enhanced the photocatalytic activity of titania, with CeO_2/TiO_2 (A) being the most active catalysts. For cerium-doped TiO_2, both the formation of labile oxygen vacancies and the relatively high mobility of bulk oxygen species have been reported. Hence, the electrons trapped in Ce^{4+}/Ce^{3+} sites can be easily transferred to oxygen on the surface of cerium-treated TiO_2 catalysts, which prohibits the electron-hole recombination and thus increases the quantum yield of photocatalysis [5]. Another factor may account for the observed high photocatalytic activity of ceria modified titania catalysts by considering the optical properties of ceria. Ceria is n-type semiconductor with band gap energy equal to 2.94 eV (lower than that of titania) and consequently it can be activated by irradiation with light in the near UV–Vis range. Thus it can expand the light absorption range of titania.

CONCLUSIONS

The following are the main conclusions that may be drown from the obtained results:

- Single and mixed phase titania was synthesized by microwave assisted sol gel method. The crystallite sizes of the prepared titania solids were lower than 10 nm as determined from XRD analysis and confirmed by TEM. The microwave assisted sol gel method adopted in this study, besides saving time and energy, allow the control of phase composition and crystallite size of titania by simply controlling the concentration of Ti precursor in solution.
- Modification of the prepared titania by ceria was carried out by employing deposition- precipitation method followed by microwave irradiation for 2 minutes.
- The prepared solids have high specific surface areas and possessed mesoporous structures.
- The mixed phase titania showed better adsorption for MB dye and exhibited higher intrinsic photocatalytic activity than anatase probably due to a synergistic effect.
- Ceria modified titania exhibited higher photocatalytic activity than the pure titania.

REFERENCES

1. Ding, K., Z. Miao, B. Hu, G. An, Z. Sun, B. Han and Z. Liu, 2010. Study on the anatase to rutile phase transformation and controlled synthesis of rutile nanocrystals with the assistance of ionic liquid. Langmuir, 12(26): 10302-10294.
2. Iliev, V., D. Tomova, R. Todorovska, D. Oliver, L. Petrov, D. Todorovsky and M. Uzunova-Bujnova, 2006. Photocatalytic properties of TiO_2 modified with gold nanoparticles in the degradation of oxalic acid in aqueous solution. Appl. Catal. A, 313: 115-121.
3. Yu, J. and B. Wang, 2010. Effect of calcinations temperature on morphology and photoelectrochemic properties of anodized titanium dioxide nanotube arrays, Appl. Catal., B, 94: 295-302.
4. Liu, Z., X. Zhang, S. Nishimoto, M. Jin, D. Tryk, T. Murakami and A. Fujishima, 2007. Anatase TiO_2 nanoparticles on rutile TiO_2 nanorods: A heterogeneous nanostructure via layer-by-layer assembly. Langmuir, 23: 10916-10919.
5. Zhang, Y., A. Yuwono and J. Wang, J. Li, 2009. Enhanced photocatalysis by doping cerium into mesoporous titania thin films. J. Phys. Chem. C, 113: 21406-21412.
6. Du, P., A. Bueno-Lopez, M. Verbaas, A. Almeida, M. Makkee, J. Moulijn and G. Mul, 2008. The effect of surface OH-population on the photocatalytic activity of rare earth-doped P25-TiO_2 in methylene blue degradation. J. Catal., 260: 75-80.
7. Li, W., Y. Zhao, S. Yuan, L. Shi, Z. Wang, J. Fang and M. Zhang, 2012. Synthesis and characterization of highly dispersed TiO_2 nanocrystal colloids by microwave-assisted hydrothermal method, J. Mater. Sci., 47: 7999-8006
8. He, Z., W. Que, Y. He, J. Chen, H. Xie and G. Wang, 2012. Nanosphere assembled mesoporous titanium dioxide with advanced photocatalyatic activity using absorbent cotton as template, J. Mater. Sci., 47: 7210-7216.
9. Jung, H.S., H. Shin, J, R. Kim, J.Y. Kim and K.S. Hong, 2004. In situ observation of the stability of anatase nanoparticles and their transformation to rutile in an acidic solution. Langmuir, 20: 11732-11737.
10. Murugan, A.V., V. Samuel and V. Ravi, 2006. Synthesis of nanocrystalline anatase TiO_2 by microwave hydrothermal method. Mater. Lett., 60: 479-480.

11. Addamo, M., M. Bellardita, D. Carriazo, A.D. Paola, S. Milioto, L. Palmisano and V. Rives, 2008. Inorganic gels as precursors of TiO_2 photocatalysts prepared by low temperature microwave or thermal treatment. Appl. Catal. B, 84: 742-748.
12. Glaspell, G., H.M.A. Hassan, A. Elzatahry, V. Abdalsayed and M.S.El-Shall, 2008. Nanocatalysis on supported oxides for CO oxidation. Top. Catal., 47: 22-31.
13. Hassan, H.M.A., V. Abdalsayed, A.S. Khder, K.M. Abou Zeid, J. Terner, M.S. El-Shall, S.I. Al-Resayes and A.A. El-Azhary, 2009. Microwave synthesis of graphene sheets supporting metal nanocrystals in aqueous and organic media. J. Mater. Chem., 193: 3832-3837.
14. Zhang, P., S. Yin and T. Sato, 2009. Synthesis of high-activity TiO_2 photocatalyst via environmentally friendly and novel microwave assisted hydrothermal process. Appl. Catal. B, 89: 118-122.
15. Inada, M., A. Nishinosono, K. Kamada, N. Enomoto and J. Hojo, 2008. Microwave-assisted sol–gel process for production of spherical mesoporous silica materials. J. Mater. Sci., 43: 2362-2366.
16. Horikoshi, S. and N. Serpone, 2009. Photochemistry with microwaves catalysts and environmental applications, J. Photochem. Photobio.C, 10: 96-110.
17. Zhou, Y. and K. Fichthorn, 2012. A microscopic view of nucleation in the anatase-to-rutile transformation, J. Phys. Chem. C, 116(14): 8314-8321.
18. Cheng, H., J. Ma, Z. Zhao and L. Qi, 1995. Hydrothermal preparation of uniform nanosize rutile and anatase particles. Chem. Mater., 7: 663-671.
19. Zheng, Y., E. Shi, Z. Chen, W. Li and X. Hu, 2001. Influence of solution concentration on the hydrothermal preparation of titania crystallites. J. Mater. Chem., 11: 1547-1551.
20. Zhu, H., M. Shen, Y. Kong, J. Hong, Y. Hu, T. Liu, L. Dong, Y. Chen, C. Jian and Z. Liu, 2004. Characterization of copper oxide supported on ceria-modified anatase. J. Mol. Catal. A, 219: 155-164.
21. Zhu, H., L. Dong and Y. Chen, 2011. J. Coll. Effect of titania structure on the properties of its supported copper oxide catalysts. J. Coll. Interface Sci., 357: 497-503.
22. Zanjanchi, M., H. Golmojdeh and M. Arvand, 2009. Enhanced adsorptive and photocatalytic achievements in removal of methylene blue by incorporating tungstophosphoric acid–TiO_2 into MCM-41. J. Hazard. Mater., 169: 233-239.